

Netrin-guided accessory cell morphogenesis dictates the dendrite orientation and migration of a *Drosophila* sensory neuron

Eli M. Mrkusich¹, Zalina B. Osman¹, Karen E. Bates^{1,2}, Julia M. Marchingo¹, Molly Duman-Scheel³ and Paul M. Whittington^{1,*}

SUMMARY

Accessory cells, which include glia and other cell types that develop in close association with neurons, have been shown to play key roles in regulating neuron development. However, the underlying molecular and cellular mechanisms remain poorly understood. A particularly intimate association between accessory cells and neurons is found in insect chordotonal organs. We have found that the cap cell, one of two accessory cells of v'ch1, a chordotonal organ in the *Drosophila* embryo, strongly influences the development of its associated neuron. As it projects a long dorsally directed cellular extension, the cap cell reorients the dendrite of the v'ch1 neuron and tows its cell body dorsally. Cap cell morphogenesis is regulated by Netrin-A, which is produced by epidermal cells at the destination of the cap cell process. In *Netrin-A* mutant embryos, the cap cell forms an aberrant, ventrally directed process. As the cap cell maintains a close physical connection with the tip of the dendrite, the latter is dragged into an abnormal position and orientation, and the neuron fails to undergo its normal dorsal migration. Misexpression of *Netrin-A* in oenocytes, secretory cells that lie ventral to the cap cell, leads to aberrant cap cell morphogenesis, suggesting that Netrin-A acts as an instructive cue to direct the growth of the cap cell process. The netrin receptor Frazzled is required for normal cap cell morphogenesis, and mutant rescue experiments indicate that it acts in a cell-autonomous fashion.

KEY WORDS: Netrin, Frazzled, Dendrite growth, Cap cell, Neuron migration, Chordotonal organ, *Drosophila*

INTRODUCTION

The developmental processes of cell migration and dendrite and axon growth are driven by marked changes in cell morphology, which are in turn the product of tightly orchestrated alterations in cytoskeletal organisation. The same set of cytoskeletal components is employed for this purpose in both migrating cells and growing neurites. In addition, many of the extracellular cues that guide axons and dendrites along specific pathways also guide migrating cells. The slits, netrins, ephrins and semaphorins are examples of families of molecules that perform guidance roles in both situations (Cirulli and Yebra, 2007; Knoll and Drescher, 2002; Kruger et al., 2005; Steigemann et al., 2004; Wang et al., 2003). Many questions remain about how guidance molecules function in these diverse settings. These issues are well illustrated by the netrins, a family of secreted proteins, which regulate axon growth, dendrite morphogenesis and cell migration in both vertebrates and invertebrates (Bradford et al., 2009). Netrins elicit diverse, and in some cases opposing, cellular responses, depending on the developmental context, raising the question of how this single class of molecules can

exert such different effects. The netrin receptor Frazzled (Fra), the *Drosophila* homologue of DCC/UNC-40, can act either in a cell-autonomous fashion in the netrin-responding cell or non-cell-autonomously by localising netrin distribution (Bhat et al., 2007; Garbe and Bashaw, 2007; Hiramoto and Hiromi, 2006; Hiramoto et al., 2000).

Many neurons develop in close association with other non-neuronal cell types. Such cells, which can be collectively termed 'accessory cells', have been shown to play key roles in regulating the differentiation of their associated neurons (Freeman, 2006). A particularly intimate association between neurons and accessory cells is seen in insect chordotonal organs. These sense organs consist of a bipolar neuron and three lineage-related accessory cells: the scolopale cell, which ensheathes the neuron's dendrite, and the cap and ligament cells, which attach to opposite sides of the neuron and tether the organ to the epidermis (Hartenstein, 1988). The chordotonal neuron is highly polarised, with its axon and single dendrite emerging from opposite sides of the cell body at stereotypic locations. The dendrite develops in close association with the scolopale cell, growing through a lumen that develops within this cell (Carlson et al., 1997a). The cap cell is tightly connected to the dendrite via the cap matrix and to the scolopale cell via septate junctions (Carlson et al., 1997b). This physical coupling allows movements of the body wall to be conducted to the dendrite, providing a stretch receptor function for the organ. The close association between the scolopale and cap cells and the dendrite during development raises the possibility that these accessory cells play a role in regulating dendrite morphogenesis, although no evidence to support this idea has emerged to date. Unlike other insect sense organs, some chordotonal organs – e.g. the lch5 cluster and v'ch1 organs in the abdomen of the *Drosophila*

¹Department of Anatomy and Cell Biology, University of Melbourne, VIC 3010, Australia. ²Department of Zoology, University of Hawaii, Honolulu, HI 96822, USA.

³Department of Medical and Molecular Genetics, Indiana University School of Medicine-South Bend and Department of Biological Sciences, University of Notre Dame, Raclin-Carmichael Hall, 1234 Notre Dame Avenue, South Bend, IN 45517, USA.

*Author for correspondence (p.whittington@unimelb.edu.au)

embryo – undergo a substantial change in position after birth. Little is known about how this migration is regulated at either cellular or molecular levels.

We have used the *Drosophila* v'ch1 sense organ as a model to investigate the role that accessory cells play in regulating the development of their associated neuron. We have demonstrated that the cap cell undergoes a marked morphogenetic change soon after birth, extending a process that attaches to the epidermis in the dorsal body wall. The dorsal process is guided by Netrin-A, produced in epidermal cells at its future site of attachment. Furthermore, we find that cap cell morphogenesis has a pronounced effect on the chordotonal neuron, both aligning its dendrite into a stereotypic orientation and towing its cell body into its final position in the dorsal body wall. In the absence of Netrin-A activity, the v'ch1 cap cell grows towards the attachment site of a different chordotonal organ and, in doing so, pulls the v'ch1 dendrite into an aberrant ventral orientation.

MATERIALS AND METHODS

Fly strains

w¹¹¹⁸, *NetA^{BG022098}* (*NetA^P*), *NetB^{KG01368}* (*NetB^P*) and *UAS-CD8-GFP* *Drosophila* lines were obtained from Bloomington Stock Centre. *NetA^P* is a *p*-element insertion into the first exon of *NetA* and is probably a null allele, based on lack of staining with a *NetA* riboprobe (data not shown). *Netrin^{Df(1)NP5}*, which removes both *NetA* and *NetB* was provided by Akira Chiba. The *NetA^A* and *NetB^A* *p*-element excision lines as well as the *UAS-NetA* transgene were provided by Barry Dickson. *elav-GAL4* drives expression in all of the sensory neurons and the scolopale cells of the lch5 organ. In rare cases, *elav-GAL4* also drives expression in the v'ch1 cap cell. *P0163-GAL4* is expressed in all post-mitotic sensory neurons and their support cells (Hummel et al., 2000). *MZ97-GAL4*, provided by Gerd Technau, drives expression in oenocytes from stage 13 (von Hilchen et al., 2008). *spalt-GAL4* (*sal-GAL4*) drives expression in the dorsal epidermis, trachea, oenocytes and scolopale cells from stage 13 (Kühnlein and Schuh, 1996; Rusten et al., 2001).

Immunohistochemistry

Embryos were collected at 25°C, or at 29°C for experiments using GAL4 driver lines. Embryos were staged based on dorsal closure and gut morphology (Campos-Ortega and Hartenstein, 1985) and were stained using standard immunohistochemical methods (Patel, 1994). MAb22C10 (anti-Futsch), anti-Prospero (Vaessin et al., 1991) and E7 anti- β -tubulin were supplied by the Developmental Studies Hybridoma Bank. Anti- β -galactosidase was purchased from Promega (Madison, WI, USA). Primary antibodies were diluted in phosphate buffer saline containing 0.1% Tween-20 (PBT) plus 5% normal goat serum (NGS) at 1:10 for MAb22C10, anti-Prospero and E7 anti- β -tubulin and 1:250 for anti- β -galactosidase. Appropriate HRP-conjugated secondary antibodies were used at 1:500 dilution and visualised using diaminobenzidine, with or without nickel intensification. Stained embryos were mounted in 70% glycerol in PBS. Projections of in-focus digital images in multiple focal planes were made using CombineZP image stacking software by Alan Hadley.

For immunofluorescence, Cy5-conjugated goat anti-HRP (Jackson Immunologicals, West Grove, Pennsylvania, USA) was used at 1:100. Alexa-488 conjugated anti-mouse IgG (obtained from Chemicon, Sydney, NSW, Australia) was used at 1:500. Embryos were mounted in Vectashield (Vector Labs, Burlingame, CA, USA) and examined using Zeiss LMS 510 META or LMS5 Pascal confocal microscopes. *z*-series were projected to obtain cross-sectional views using ImageJ v1.42 (NIH) software.

In situ hybridisation

The Patel (Patel, 1996) protocol for combined detection of mRNA and protein in *Drosophila* embryos was used for *NetA*/MAb22C10 double-label experiments. This protocol was modified slightly, as described in Duman-Scheel et al. (Duman-Scheel et al., 2002), Patel et al. (Patel et al., 2001) and VanZomeran-Dohm et al. (VanZomeran-Dohm et al., 2008).

DiI labelling

Individually identified sensory neurons were labelled with DiI by juxtacellular injection as previously described (Merritt and Whittington, 1995). Homozygous mutant embryos were genotyped by selection against GFP expression from a balancer chromosome before dye injection. Stained neurons were photoconverted in the presence of 0.2% diaminobenzidine to give a permanent dark reaction product.

Measurements and statistical analysis

All measurements were performed using ImageJ v1.42 (NIH) software. The centre of the v'ch1 neuron soma was defined as the midpoint of a line along the longest axis of the cell body. The angle between the anteroposterior axis of the embryo and a line connecting the centre of the cell and the site of exit of the dendrite was used to quantify the exit site of the dendrite. The angle between the axis of the dendrite and the anteroposterior axis was used to quantify dendrite orientation. The distance between the most dorsal edge of the v'ch1 cell body and the dorsal edge of the lch5-5 neuron cell body was used to quantify position of the v'ch1 cell. Measurements are expressed as mean \pm circular standard deviation (s.d.). The position of the v'ch1 neuron in different genotypes was compared using a one-way ANOVA followed by a post-hoc Tukey's test using Prism 5 (GraphPad Software, San Diego, CA, USA). Analysis of circular data was performed using Oriana 2 software (Kovach Computing Services, Anglesey, Wales, UK). The Rayleigh test was used for circular uniformity. Watson's U^2 test was used to compare distributions of site of exit and dendrite direction between genotypes. Fisher's exact test was used to compare penetrance levels of axon pathway and cap cell defects in different genotypes.

Time-lapse microscopy

Embryos were dechorionated in bleach and mounted in halocarbon oil (Sigma-Aldrich, Sydney, NSW, Australia) under a coverslip. Imaging was performed with a Leica TCS SP5 inverted confocal microscope using a 63 \times /1.4 oil lens. Images were captured as 512 \times 512 pixel *z*-series every 3 minutes. *z*-series were projected using Leica LAS AF software. Development under imaging conditions proceeds at approximately half the rate of normal development. All cells appeared healthy and in their correct spatial arrangement at the end of the time-lapse period.

RESULTS

Netrin-A regulates v'ch1 dendrite position, orientation and neuron migration

We used mAb22C10 immunostaining to reveal the cell body position and dendrite and axon morphology of the v'ch1 neuron in wild-type and Netrin mutant embryos. The site of exit of the dendrite and axon from the v'ch1 cell body and their orientation lie within a narrow range in stage 16 wild-type embryos (Fig. 1A-C, Fig. 2).

Stage 16 hemi/homozygous *NetA^P* and *NetA^A* embryos show obvious defects in v'ch1 dendrite growth. Although the dendrite has an apparently normal morphology, it emerges from an abnormal position from the soma and projects in an aberrant direction (Fig. 1D-F, Fig. 2). Measurements of the site of exit of the dendrite in the *NetA* mutant show that this parameter is random if dendrites within the wild-type range are excluded ($P>0.05$), whereas the dendrite orientation shows a distinct ventral bias (mean angle $294.3\pm19.5^\circ$, $P<0.05$). The penetrance of these dendrite defects is high: in the *NetA^P* mutant, the site of dendrite exit and dendrite orientation lies outside the wild-type range in 57.6 and 70.5% ($n=61$) of v'ch1 neurons, respectively. v'ch1 is apparently the only sensory neuron that shows an aberrant dendritic morphology in *NetA* mutants.

Growth of the v'ch1 axon, unlike the dendrite, is virtually unaffected in *NetA* mutants. The site of exit of the axon in all embryos examined is within the wild-type range at all stages from

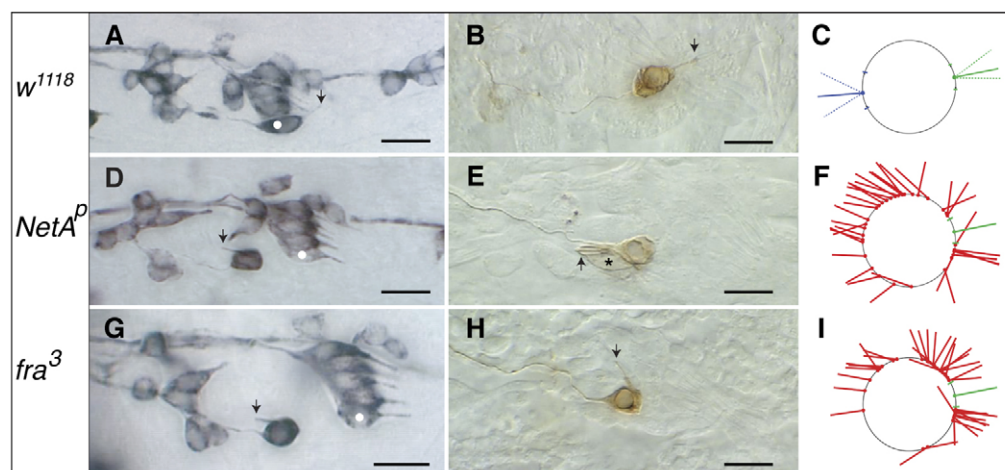


Fig. 1. *Netrin-A* and *frazzled* mutant *Drosophila* embryos show defects in v'ch1 dendrite position and orientation. (A-I) Single hemisegments of mAb 22C10-immunostained embryos (A,D,G), Dil-labelled v'ch1 neurons (B,E,H) and diagrams showing site of exit and orientation of the v'ch1 dendrite in wild-type (C), *NetA^P* (F) and *fra³* (I) mutants. Arrows in A, D and G show the v'ch1 dendrite, white dots show the lch5-5 neuron, and the asterisk in E shows the v'ch1 scolopale cell. (C) The mean and range of dendrite exit position (green dot and dashes on circle, representing the v'ch1 cell body) and orientation (unbroken and broken green lines, respectively) in wild-type embryos ($n=41$) are shown. Equivalent positions and orientations for the axon are shown in blue. (F,I) Each red line in these diagrams represents the site of exit and orientation of individual dendrites that lie outside the wild-type range of positions and orientations (green). In this and all subsequent figures anterior is up and dorsal is to the right. Scale bars: 10 μ m.

stage 14 to 16 (see Fig. S1 in the supplementary material). The consistent position of the axon at these developmental stages in the *NetA* mutant excludes the possibility that the dendrite orientation defects are simply a consequence of rotation of the entire neuron. Furthermore, in 95% of cases the axon follows a normal trajectory into the segmental nerve. Single cell labelling by DiI injection of the v'ch1 neuron in wild-type and *NetA* mutants (Fig. 1B,E) confirms that, despite their aberrant orientation, dendrites in mutant embryos possess a normal morphology with an inner and outer segment (Hartenstein, 1988) and that the v'ch1 axon projects into the central nervous system along its normal pathway, the segmental nerve ($n=7$).

To determine at which developmental stage these defects first become apparent, we immunostained wild-type and *NetA* mutant embryos with mAb22C10. Late stage 12/early stage 13 wild-type embryos show an early stage of v'ch1 dendrite growth: the dendrite takes the form of a small conical protrusion on the anterodorsal side of the soma, directed superficially towards the epidermis (Fig. 3A). As the dendrite extends from stages 13 to 15, it adopts a rod-like shape (Fig. 3B,C) and progressively moves into a position in which its long axis is almost parallel to the plane of the epidermis (Fig. 3E-G). The mean site of exit of the v'ch1 dendrite from the soma and its orientation do not change from stage 13 to stage 16. However, there is a higher degree of variability in these parameters at stage 13 than at stage 16 ($P<0.05$, Fig. 4A). As development proceeds, the position and orientation of the v'ch1 dendrite is progressively refined through to stage 15, when its mature position and orientation are achieved.

Stage 13-14 *NetA* embryos show no significant difference from wild-type embryos of the same stages in the site of exit of the v'ch1 dendrite or its orientation (Fig. 4B, $P>0.05$). However, the refinement in dendrite position and orientation, which takes place in wild-type embryos between stages 13 and 15, does not occur in *NetA* mutant embryos: the site of dendrite exit shows the same variability at stage 15 as in earlier stages. Furthermore, a number

of dendrites in stage 15 mutant embryos display an aberrant site of exit and ventral orientation, a defect that becomes much more frequent by stage 16.

Another obvious defect seen in *NetA* mutants is a failure of v'ch1 neuron migration. In wild-type embryos, v'ch1 begins to migrate dorsally between stages 14 to 15 and by stage 16 has reached a position dorsal to the lch5 cluster (Fig. 3A-D, Fig. 5A). There is considerable variability in the timing of v'ch1 migration in wild-type embryos – some neurons in stage 15 embryos have not begun to migrate, while others have reached the lch5 cluster.

The range of v'ch1 neuron positions in stage 16 hemi/homozygous *NetA^P* and *NetA^D* embryos differs significantly from wild-type embryos ($P<0.001$, Fig. 5B). The average position of v'ch1 neurons in these embryos is the same as in stage 13-14 mutant and wild-type embryos, indicating that v'ch1 neuron migration fails to commence in the mutants. There is a high correlation between migratory and dendrite defects: 85% of v'ch1 neuron that had failed to migrate had dendrite site of exit defects, whereas 100% of neurons with site of exit defects had failed to migrate. In addition to these defects in dendrite morphology and cell migration, the v'ch1 cell body in *NetA* mutant embryos possesses a rounded shape rather than the elliptical shape evident in wild-type embryos from stage 15 onwards (compare v'ch1 in Fig. 1D with Fig. 3D).

We have seen both v'ch1 dendrite and neuron migration defects in the deficiency line *Netrin^{Df(1)NP5}* (Mitchell et al., 1996), which removes both *NetA* and *NetB*: v'ch1 dendrite exit points and orientations and cell body positions show a similar distribution to the *NetA* mutants (Fig. 2, Fig. 5B). However, hemi/homozygous *NetB^P* and *NetB^D* mutant embryos show values for v'ch1 dendrite location, orientation and neuron cell body position that are not significantly different from wild-type embryos ($P>0.05$, Fig. 2, Fig. 5B). We conclude that *NetA*, but not *NetB*, is required for normal development of the v'ch1 dendrite and for dorsal migration of the v'ch1 neuron.

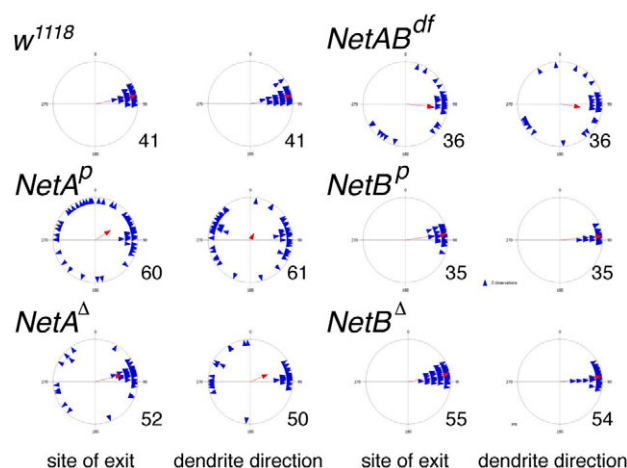


Fig. 2. Patterns of v'ch1 dendrite growth in *Netrin* mutant *Drosophila* embryos. Each blue triangle in these scatter plots shows the values for an individual dendrite, and the red arrow shows the mean value for that parameter (r value). n values are indicated to the right of each plot.

***Netrin-A* mediates its effects on dendrite development and neuron migration via the *frazzled* receptor**

In order to determine whether *NetA* is mediating its effect on dendrite morphogenesis and neuron migration via the *Netrin* receptor *Frazzled*, stage 16 embryos homozygous for the loss-of-function mutations *fra*³ or *fra*⁴ were stained by mAb22C10 immunohistochemistry. These embryos show the same v'ch1 defects – aberrant dendrite position and orientation and failure of neuron migration – as *NetA* mutants (Fig. 1G–I, Fig. 5D, Fig. 6). The similarities in the *fra* and *NetA* mutant phenotypes strongly suggest that *Netrin-A*–*Frazzled* signalling is mediating dendrite position and orientation and migration of v'ch1. DiI labelling of individual v'ch1 neurons in stage 16 *fra*³ mutants (Fig. 1H) confirmed that, like the *NetA* mutants, mislocated dendrites possess a normal morphology, with inner and outer segments. Twelve of the 14 injected cells had normal axon morphology: aberrant axon projections towards the intersegmental nerve (ISN) were seen in two cases.

Our analysis of fixed *NetA* and *fra* mutant embryos suggested that the dendrite gradually moves into an aberrant position after initially exiting the cell body from a normal position. To provide a direct confirmation of this change and to better understand the dynamics of dendrite growth, we used the *elav*-GAL4 driver line to express a membrane-targeted form of GFP in the v'ch1 neuron in a *fra*³ homozygous mutant background and performed time-lapse microscopy on these embryos.

As suggested by our observations on fixed embryos, the v'ch1 dendrite initially grew out in a normal fashion in *fra* mutant embryos: the site of exit and orientation was within the wild-type range ($n=19$). However, as development proceeded, the v'ch1 neuron failed to migrate dorsally in 14 out of 19 cases. In four of these stalled cells, the v'ch1 dendrite showed a major change during the course of the imaging, progressively moving from a normal to an aberrant position and orientation (see Movie 1 in the supplementary material).

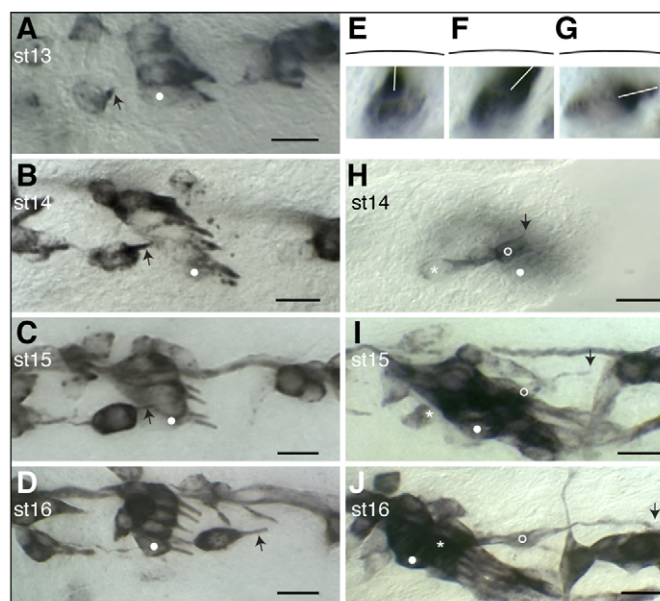


Fig. 3. Morphogenesis and migration of the v'ch1 neuron and cap cell in wild-type *Drosophila* embryos. Single hemisegments of embryos were fixed at the developmental stage indicated. (A–G) mAb22C10-stained embryos showing v'ch1 dendrite morphology (arrow). (H–J) P0163-GAL4; UAS-*tau-lacZ* embryos stained with anti- β -galactosidase, showing morphology of the v'ch1 neuron (asterisk) and cap cell (open circle). White dots in A–D and H–J show the position of the lch5-5 neuron. The arrow in H–J shows the dorsal edge/tip of the v'ch1 cap cell. (E–G) Cross-sectional views of v'ch1 reconstructed from a z-series of images. The black line shows the position of the epidermis. The white line shows the dendrite direction. Scale bars: 10 μ m.

Cap cell morphogenesis directs v'ch1 dendrite orientation and neuron migration

To determine whether the v'ch1 dendrite and cell migration defects seen in *NetA* and *fra* mutant embryos are caused by aberrant development of the v'ch1 accessory cells, we examined the morphology of these cells in wild-type, *NetA* and *fra* mutant embryos. Whereas chordotonal organs generally possess three accessory cells – ligament, scolopale and cap cells – the v'ch1 organ appears to lack a ligament cell. We base this conclusion on previously published data, which show an absence of a stained cell in the expected position of a v'ch1 ligament cell in embryos stained with anti-Reversed polarity (von Hilchen et al., 2008) and anti- β -tubulin antibodies (Inbal et al., 2003): both of these antibodies consistently stain ligament cells of other chordotonal organs.

We used anti-Prospero immunohistochemistry to label v'ch1 scolopale cell nuclei in *NetA* mutant embryos. The scolopale cell showed its normal close association with the dendrite in *NetA* mutant embryos, whether the dendrite was oriented in a normal dorsal or aberrant ventral direction (Fig. 7A,D, $n=60$). DiI injections of the v'ch1 scolopale cell in *NetA* mutants showed that it possessed a normal morphology (Fig. 1E).

To visualise normal cap cell morphogenesis, we used the P0163-GAL4 line to drive *tau-lacZ* expression in all cells comprising the v'ch1 organ followed by anti- β -galactosidase immunohistochemistry. At stage 13, the v'ch1 neuron, scolopale cell and cap cell lie in a dorsoventral row and each of these cells has a similar, simple morphology. During stage 14, a lamellipodial process forms on the dorsal edge of the cap cell (Fig. 3H). By stage

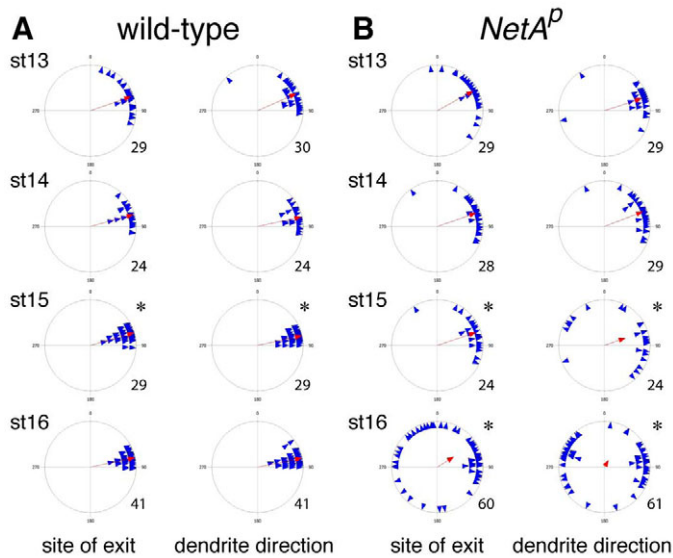


Fig. 4. Refinement of v'ch1 dendrite position and orientation does not occur in *Netrin-A* *Drosophila* embryos. Each blue triangle in these scatter plots shows the values for an individual dendrite, and the red arrow shows the mean value for that parameter (r value). n values are indicated to the right of each plot. (A) Asterisks indicate that the distributions at stage 15 are significantly different from previous stages (Watson's U^2 test, $P<0.05$). (B) Asterisks indicate that the distributions at stage 15 and 16 are significantly different from wild-type at equivalent stages (Watson's U^2 test, $P<0.05$).

15, this process has transformed into a thin, elongated cellular extension (Fig. 3I), which reaches its ultimate insertion point on the dorsal body wall by stage 16 (Fig. 3J). By this stage, the cap cell nucleus has migrated dorsally into the dorsal process.

Cap cells in stage 16 wild-type, *NetA*^Δ, *NetAB*^{Df}, *fra*³ and *fra*⁴ embryos were visualised by anti-β-tubulin immunohistochemistry. Although β-tubulin expression is not confined to the cap cell, the characteristic morphology of this cell enabled it to be readily identified. In all mutant embryos, those hemisegments in which the v'ch1 neuron had migrated dorsally consistently displayed a normal cap cell morphology: one end of the cell was attached to the tip of the v'ch1 dendrite, whereas the other was attached to the epidermis, just anterior to cells in the dorsal sensory neuron cluster. In those hemisegments in which the v'ch1 neuron had failed to migrate dorsally, the cap cell retained its close association with the dendrite, but was shorter and wider than normal and was oriented in an aberrant anteroventral direction (Fig. 7E). The orientation of the cap cell was relatively consistent in such hemisegments, whereas its associated dendrite showed a highly variable position and orientation (see Fig. S2 in the supplementary material). The ventral insertion point of the aberrant cap cell was also quite consistent, lying close to the epidermal attachment site of the cap cell of the vchB chordotonal organ, which in turn lies close to the ventral attachment sites of the lateral transverse muscles, 21 and 22 (Fig. 7E, see Fig. S2 in the supplementary material). The penetrance of the defective cap cell morphology phenotype was similar in *NetA*^Δ, *NetAB*^{Df}, *fra*³ and *fra*⁴ embryos (Table 1). These observations strongly suggest that the defects in v'ch1 dendrite position and orientation seen in *NetA* and *fra* mutants result from defective cap cell morphogenesis. They also suggest that, in the absence of its normal NetA guidance cue, the

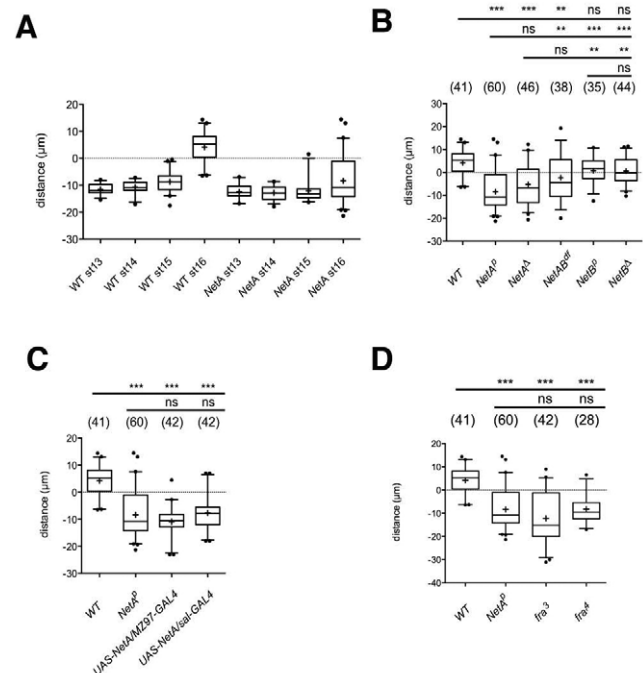


Fig. 5. Failure of v'ch1 neuron migration following loss of function or mis/overexpression of *Netrin-A* or *frazzled*.

(A–D) Data in boxplot format (+, mean; middle line, median; box, 25–75% quartiles; error bars, data within 5–95% range; dots, outliers) showing the distance between v'ch1 and lch5-5 neuron cell bodies in: (A) wild-type and *NetA* mutant embryos at various developmental stages; (B) wild-type and various *NetA* and *NetB* mutant embryos at stage 16; (C) wild-type, *NetA* mutant and *NetA* misexpression embryos at stage 16; (D) wild-type, *NetA*^P, *fra*³ and *fra*⁴ mutant embryos at stage 16. A negative value indicates that v'ch1 lies ventral to lch5-5, a positive value that it lies dorsal. Annotations above the charts in B–D indicate whether the value for the genotype beneath is significantly different to that of the genotype on the far left of the accompanying line (***, $P<0.001$; **, $P<0.01$; ns, not significant; one-way ANOVA followed by Tukey's post-test comparison). n values for each genotype are shown in brackets.

v'ch1 cap cell responds to the same cue that normally guides the growth of the vchB cap cell. This alternative cue is unlikely to be Netrin-B, as the cap cell of vchB is unaffected in *NetAB*^{Df} mutant embryos.

We next performed time-lapse microscopy on living wild-type and *fra* mutant embryos, using the *P0163-GAL4* driver line to drive expression of *UAS-CD8-GFP*. Live cell imaging directly reveals the highly dynamic changes in cap cell morphology in wild-type embryos inferred from the observations on fixed embryos, including the formation of a lamellipodium (see Fig. S3 in the supplementary material) and its rapid transformation into a thin cellular process (see Fig. S4 in the supplementary material). The tip of the dorsal process has a morphology and behaviour similar to that of a neuronal growth cone, with filopodia radiating in multiple directions. These time-lapse observations confirm that translocation of the nucleus into the dorsal process is a relatively late event in cap cell morphogenesis. They also reveal that extension of the cap cell process takes place well in advance of the beginning of migration of the v'ch1 neuron, supporting the view that the neuron does not actively migrate dorsally, but rather is passively towed by the cap cell. The relative timing of events

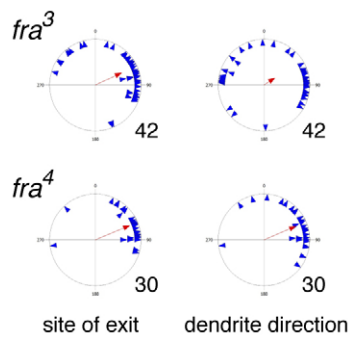


Fig. 6. Patterns of v'ch1 dendrite growth in *frazzled* mutants.

Each blue triangle in these scatter plots shows the values for an individual dendrite, and the red arrow shows the mean value for that parameter (r value). n values are indicated to the right of each plot.

suggests that the normal refinement in position of the v'ch1 dendrite is the result of a pulling force exerted on the dendrite tip by the extending cap cell.

Live cell imaging of *fra* mutant embryos showed that in seven out of 16 hemisegments, cap cells failed to extend a dorsal process and instead produced an aberrant ventrally directed process. In one case, the cap cell initially formed a dorsal process, but this process did not continue to extend, and the cell subsequently extended a ventral process. Ventrally directed cap cell processes were invaded by the cap cell nucleus, thereby moving the cell into an inappropriate, ventral position (see Movie 2 in the supplementary material). The scolopale cell does not initially change position as the cap cell takes up a new position. Given that the scolopale cell ensheathes the dendrite, this provides support for the view that the repositioning of the dendrite observed in late stage *NetA* and *fra* mutants is a consequence, rather than a cause of aberrant cap cell morphogenesis.

In summary, our observations of the behaviour of cells in the v'ch1 organ in both fixed and living embryos strongly suggest that the dorsal extension of the cap cell, followed by invasion of the nucleus into this process, is responsible for pulling the v'ch1 neuron cell body into a more dorsal position during normal development and for reorienting its dendrite into a stereotypic position and direction. A pulling force exerted by the cap cell on the neuron also provides a ready explanation for the dorsoventral lengthening of the v'ch1 neuron cell body seen during normal development. Similarly, the migration of the cap cell into an aberrant ventral position in *NetA* and *fra* mutants can account for the failure of v'ch1 neuron migration, abnormal dendrite position and orientation and a rounded neuron cell body shape (see Fig. S5 in the supplementary material). In the occasional hemisegment in mutant embryos, the cap cell morphology is abnormal, whereas the dendrite exit position is within the wild-type range. We suggest that this reflects an intrinsic variability in the pulling force exerted by the mislocated cap cell on the dendrite.

Misexpression of *Netrin-A* results in defective v'ch1 cap cell morphogenesis and failed neuron migration

If *NetA* acts as an instructive guidance cue for cap cell growth, misexpression of *NetA* should result in aberrant cap cell morphogenesis. As a prelude to this experimental intervention, we sought to establish the normal *NetA* expression pattern by in situ

hybridisation. Consistent with an earlier report (Mitchell et al., 1996), we found that in stage 13-14 embryos, *NetA* is expressed in a patch of epidermis, which lies just anterior to the most ventral cells in the dorsal sensory neuron cluster (see Fig. S6 in the supplementary material). The future site of insertion of the v'ch1 cap cell process lies in the middle of this patch of *NetA* expression. The dorsal edge of the cap cell is at this early stage close to, but physically separated from, the ventral limit of *NetA* expression. Sensory neurons, their accessory cells and neighbouring internal cells such as oenocytes show no detectable signs of *NetA* expression. The location of *NetA* expression is consistent with the idea that it acts as an instructive cue to guide the growth of the dorsal process of the v'ch1 cap cell.

We expressed a wild-type *NetA* transgene in an ectopic location using two GAL4 lines: *sal*-GAL4 and *MZ97*-GAL4. These lines drive expression in the larval oenocytes, which lie immediately internal to the v'ch1 neuron and ventral to its cap cell. We found that in 20/24 hemisegments the cap cell failed to form a long dorsal process (Fig. 7I). The defective cap cells displayed a range of morphologies, possessing either: a shortened dorsal process that had not extended beyond the *lch5* scolopale cells, a ventrally directed process, or both a ventral and dorsal process (see Fig. S8 in the supplementary material). The ventrally directed processes had not extended as far as in *NetA* mutants and had not been invaded by the cap cell nucleus (compare Fig. 7E to 7I). The cap cell soma in these embryos was found in the epidermal cell layer and had thus failed to delaminate (Fig. 7G). The cap cell processes were restricted to the region around the oenocytes, in which *NetA* had been ectopically expressed (Fig. 7G,I).

In all hemisegments with a defective cap cell morphology, the v'ch1 neuron cell body had failed to migrate dorsally (Fig. 5C), whereas v'ch1 dendrite position, orientation and morphology appeared to be unaffected (see Fig. S7 in the supplementary material).

The aberrant pattern of process extension seen in the v'ch1 cap cell when *NetA* is ectopically expressed supports the view that *NetA* acts as instructive cue to direct the extension of the cap cell process. The absence of v'ch1 dendrite defects in this experimental setting can be explained by the fact that, unlike in the *NetA* mutant, there is no translocation of the cap cell soma to an aberrant ventral position: thus the dendrite is not pulled into an abnormal position or orientation. Apparently, extension of the cap cell process in an aberrant direction without an accompanying movement of the soma in that direction does not generate a sufficient force for reorientation of the dendrite. However, the failure of the cap cell to extend dorsally does lead to v'ch1 neuron stalling.

frazzled apparently acts cell-autonomously to regulate cap cell morphogenesis

We used in situ hybridisation to determine the normal pattern of *fra* mRNA expression in the periphery. Consistent with a previous report (Kolodziej et al., 1996), we found that *fra* is expressed in a widespread fashion in the epidermis of the body wall and in peripheral neurons. We also observed expression in the accessory cells of the chordotonal organs, including the ligament, scolopale and cap cells (data not shown).

To shed light on where *fra* activity is required for normal cap cell morphogenesis, we attempted to rescue the *fra*³ mutant phenotypes using either *elav*-GAL4 or *P0163*-GAL4 lines to drive expression of a wild-type *fra* construct. As noted above, *elav*-GAL4 drives expression in the scolopale cells of the *lch5* cluster in addition to all of the sensory neurons, but only rarely drives

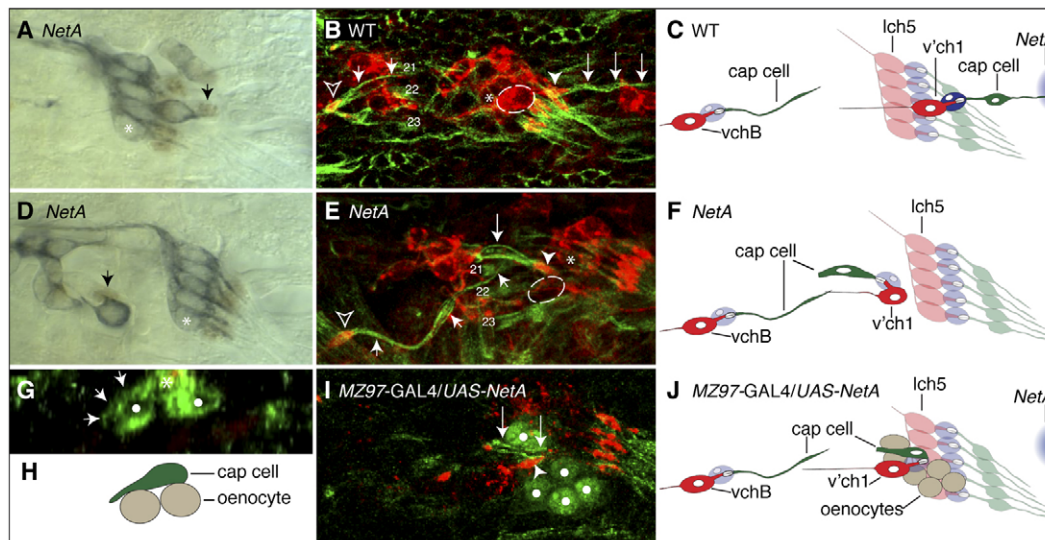


Fig. 7. Aberrant morphogenesis of v'ch1 cap cell following loss of function or misexpression of *Netrin-A*. Images of stage-16 *Drosophila* embryos with the genotypes indicated. (A,D) The scolopale cell nucleus (arrow) is revealed by anti-Prospero immunohistochemistry (brown), and sensory neurons are labelled with mAb 22C10 (blue). The scolopale cell associates closely with the dendrite, whether it is in a normal (A) or aberrant (D) position. (B,E) Cap cells are stained with anti- β -tubulin (green) and neurons with anti-HRP (red). The v'ch1 neuron in the *NetA* embryo in E (outlined, not included in projection for sake of clarity) has stalled ventral to the lch5 cluster (asterisk); compare with its normal position in the wild-type embryo (B). The cap cell (large arrows) retains its association with the v'ch1 dendrite (arrowhead) in the mutant, but it is oriented anteroventrally and attaches to the epidermis near the cap cell of vchB (small arrows), close to the muscle 21 and 22 attachment sites. The vchB dendrite in B and E is indicated by an open arrowhead. (G,I) *NetA* was ectopically expressed in oenocytes (white dots) using the MZ97-GAL4 driver line. (G) A transverse view reveals that the cell body of the v'ch1 cap cell (asterisk) has remained in the epidermal layer, directly superficial to the oenocytes and has extended an aberrant ventral process (arrows) along the surface of an oenocyte. (I) The v'ch1 cap cell has projected an aberrant ventral process (arrows) but the nucleus has not translocated into this process. (C,F,H,J) Schematics of B,E,G,I are shown in C,F,H,J, respectively. The v'ch1 neuron cell body is outlined. The site of endogenous *NetA* expression is shown in blue in C and J. Scale bars: 10 μ m.

expression in the cap and scolopale cells of the v'ch1 organ. *P0163-GAL4*, by contrast, consistently drives expression in all cells of chordotonal organs, including the neuron, scolopale and cap cells.

When *fra* was expressed using the *elav-GAL4* driver, there was only a slight reduction in the penetrance of the defective cap cell morphology phenotype (Table 1), which is not statistically significant ($P > 0.05$).

In comparison, driving *fra* with *P0163-GAL4* resulted in a near complete rescue of the cap cell mutant phenotype (Table 1). The most likely interpretation of these data is that *Fra* regulates cap cell morphogenesis in a cell-autonomous fashion. However, because *P0163-GAL4* drives expression in the scolopale cell as well as the cap cell, we cannot exclude the possibility that *Fra* acts within the former cell type to direct cap cell process extension.

Table 1. Penetrance of the misoriented cap cell phenotype in *NetA*, *fra* mutant and *fra* mutant rescue embryos

Genotype	Cap cell defects	
	Penetrance (%)	<i>n</i>
<i>NetA</i> ^A	68.0	25
<i>NetA</i> ^B ^{Df}	68.0	25
<i>fra</i> ³	62.5	32
<i>fra</i> ⁴	60.7	28
<i>elav-GAL4; fra</i> ³ , <i>UAS-fra</i>	43.3	30
<i>fra</i> ³ , <i>UAS-fra; P0163-GAL4</i>	8.8***	34

Percentages of hemisegments that show ventrally directed cap cells in each genotype are indicated. *n* is the total number of hemisegments examined. Asterisks indicate *P*-values from Fisher's exact test. ****P* < 0.001.

DISCUSSION

Dorsal extension of the cap cell repositions the v'ch1 neuron and its dendrite

Many sense organs in insects are multicellular, consisting of a neuron and two or more closely associated cells, which collaborate to transduce sensory stimuli into electrical activity in the mature organ. Our study has revealed that the cap cell, one of the accessory cells of the v'ch1 chordotonal organ, also plays a key role in the morphogenesis of its associated neuron.

A number of lines of evidence suggest that dorsally directed extension of the cap cell both tows the v'ch1 neuron cell body from its birthplace into its final position in the dorsolateral region of the body wall and also pulls its growing dendrite into a stereotypic orientation. These include: the tight physical connection, which is maintained throughout development, between the cap cell and the tip of the dendrite in both wild-type and *NetA* mutant embryos; the relative timing and common direction of cap cell extension, dendrite reorientation and neuron migration observed in wild-type embryos; the tight correlation between aberrant direction of cap cell extension, failure of neuron migration and inappropriate dendrite orientation seen in *NetA*, *fra* mutants and *NetA* misexpression embryos; and the consistent failure of neuron migration when the cap cell fails to extend dorsally following misexpression of *NetA*.

The variability in v'ch1 dendrite position seen at early stages of dendrite growth in wild-type embryos probably reflects a degree of imprecision in the mechanisms that specify the initial direction of dendrite outgrowth. Whether a neuron-intrinsic cue, related to the plane of division of the neuron progenitor cell, or some external cue determines the site of dendrite emergence remains to be

determined. In any event, we can be confident that *NetA* plays no role in this early phase of dendrite growth, as it is unaffected in *NetA* mutant embryos.

The extent to which the dendrite can be relocated after it has first emerged from the v'ch1 neuron cell body in *NetA* and *fra* mutants is surprising: to our knowledge such a phenomenon of neurite repositioning has not previously been described. It implies a considerable flexibility in the cellular machinery for anchoring the base of the dendrite.

v'ch1 and the lch5 cluster are the only sensory neurons in the body wall of the *Drosophila* embryo to undergo significant movements during normal development: v'ch1 migrates dorsally, whereas the lch5 cluster moves ventrally. Our findings suggest that the v'ch1 neuron does not actively migrate into a more dorsal position: rather, it is passively towed by the cap cell. Kraut and Zinn (Kraut and Zinn, 2004) have presented a different view of chordotonal organ migration. They suggest that the chemo-repellent Slit acts directly on thoracic chordotonal neurons via Robo2 (Leak – FlyBase) receptors, blocking their response to ventral attractants that promote a ventral migration of lch5 neurons in abdominal segments. However, the chordotonal neuron migration phenotypes observed by these authors could be secondary to abnormal morphogenesis of their associated ligament and/or scolopale cells. Indeed, an earlier study has suggested that ligament cells pull the lch5 neurons from a dorsal to a ventral position (Inbal et al., 2003), and time-lapse observations we have made of lch5 migration in the current study (data not shown) support that view.

The dramatic morphogenetic changes that the cap cell undergoes during its dorsal extension provide us with a tractable model for dissecting the molecular basis for cell migration. The cap cell is large, readily visualised both in fixed and living embryos and is potentially accessible for direct surgical manipulations. It shows features of both cell migration (lamellipodial extension and nuclear translocation) and of axon growth (growth cone extension with filopodia).

Netrin-A guides dorsal outgrowth of the cap cell

The dorsally directed extension of the v'ch1 cap cell is dependent upon NetA function. In *NetA* mutants, the cap cell undergoes morphogenesis, but extends a process in a ventral, rather than a dorsal, direction. The pattern of cap cell process extension seen when *NetA* is expressed ventral to the cap cell suggests that NetA acts as an instructive guidance factor for cap cell growth. This is supported by the normal expression pattern of NetA: the final insertion point of the cap cell process is located near the middle of the patch of epidermal *NetA* mRNA expression.

In *NetA* mutants the cap grows quite consistently in an anteroventral direction and inserts at a specific location in the epidermis, close to the site of insertion of the vchB cap cell. This suggests that, in the absence of its normal guidance cue NetA, the v'ch1 cap cell is responding to the same attractive cues that guide the extending vchB cap cell. The fact that the v'ch1 cap cell can reliably grow towards this alternative location via a totally different route to that used by the vchB cap cell suggests that this cue functions as a chemoattractant.

In all of its previously described developmental roles, *NetA* appears to act redundantly to *NetB*. This generalisation does not hold for guidance of v'ch1 cap cell growth, as *NetB* appears to play no role in this process. *NetB* mutant embryos do not display cap cell defects, the phenotypes of *NetA,B* mutants are similar to *NetA*

mutants and ectopic expression of *NetB* in oenocytes, unlike *NetA*, has no effect on v'ch1 migration or dendrite growth (data not shown).

Frazzled acts cell-autonomously to guide extension of the cap cell process

In many developmental contexts, binding of Netrin to its receptor, UNC-40/DCC/Fra, directly elicits a cellular response in the cell bearing the receptor, whereas in other situations Fra acts in a non-cell-autonomous fashion (Hiramoto et al., 2000; Garbe and Bashaw, 2007).

We have found that guidance of v'ch1 cap cell growth by NetA requires Fra activity: *fra* mutants show the same dendrite and cell migration and cap cell defects as *NetA* mutants. Our *fra* mutant rescue experiments suggest that Fra regulates cap cell morphogenesis via a cell-autonomous mechanism: defective cap cell phenotypes in *fra* mutants are almost completely rescued by driving a wild-type *fra* gene construct with *P0163*-GAL4, which drives gene expression in the whole v'ch1 sense organ. By contrast, there is no significant rescue of the mutant phenotype with the neuronal driver line *elav*-GAL4, which expresses only rarely in the cap cell.

Acknowledgements

We thank Barry Dickson, Akira Chiba and Gerd Technau for fly lines, Nipam Patel for mAb 22C10 and Kevin Mitchell for *NetA* cDNA. Harishan Tharmarajah, Jutta Wellmann and Dianne Mangelsdorf provided valuable technical assistance. We thank Massimo Hilliard and two anonymous reviewers for suggested changes, which greatly improved the manuscript. Antibodies were obtained from the Developmental Studies Hybridoma Bank, developed under the auspices of the NICHD and maintained by the University of Iowa. Funding support was provided by a Melbourne University Early Career Grant to E.M.M., an Australian Research Council Discovery Grant to P.M.W. and an NIH grant (R01AI081795-01) to M.D.S. Deposited in PMC for release after 12 months.

Competing interests statement

The authors declare no competing financial interests.

Supplementary material

Supplementary material for this article is available at <http://dev.biologists.org/lookup/suppl/doi:10.1242/dev.047795/-DC1>

References

- Bhat, K. M., Gaziova, I. and Krishnan, S. (2007). Regulation of axon guidance by slit and netrin signaling in the *Drosophila* ventral nerve cord. *Genetics* **176**, 2235–2246.
- Bradford, D., Cole, S. J. and Cooper, H. M. (2009). Netrin-1: diversity in development. *Int. J. Biochem. Cell Biol.* **41**, 487–493.
- Campos-Ortega, J. A. and Hartenstein, V. (1985). The embryonic development of *Drosophila melanogaster*. Berlin: Springer Verlag.
- Carlson, S. D., Hilgers, S. L. and Juang, J. L. (1997a). First developmental signs of the scolopale (glial) cell and neuron comprising the chordotonal organ in the *Drosophila* embryo. *Glia* **19**, 269–274.
- Carlson, S. D., Hilgers, S. L. and Juang, J. L. (1997b). Ultrastructure and blood-nerve barrier of chordotonal organs in the *Drosophila* embryo. *J. Neurocytol.* **26**, 377–388.
- Cirulli, V. and Yebra, M. (2007). Netrins: beyond the brain. *Nat. Rev. Mol. Cell Biol.* **8**, 296–306.
- Duman-Scheel, M., Pirkl, N. and Patel, N. H. (2002). Analysis of the expression pattern of *Mysidium columbiae* wingless provides evidence for conserved mesodermal and retinal patterning processes among insects and crustaceans. *Dev. Genes Evol.* **212**, 114–123.
- Freeman, M. R. (2006). Sculpting the nervous system: glial control of neuronal development. *Curr. Opin. Neurobiol.* **16**, 119–125.
- Garbe, D. S. and Bashaw, G. J. (2007). Independent functions of Slit-Robo repulsion and Netrin-Frazzled attraction regulate axon crossing at the midline in *Drosophila*. *J. Neurosci.* **27**, 3584–3592.
- Hartenstein, V. (1988). Development of *Drosophila* larval sensory organs: spatiotemporal pattern of sensory neurones, peripheral axonal pathways and sensilla differentiation. *Development* **102**, 869–886.
- Hiramoto, M. and Hiromi, Y. (2006). ROBO directs axon crossing of segmental boundaries by suppressing responsiveness to relocalized Netrin. *Nat. Neurosci.* **9**, 58–66.

- Hiramoto, M., Hiromi, Y., Giniger, E. and Hotta, Y. (2000). The *Drosophila* Netrin receptor Frazzled guides axons by controlling Netrin distribution. *Nature* **406**, 886-889.
- Hummel, T., Krukkert, K., Roos, J., Davis, G. and Klambt, C. (2000). *Drosophila* Futsch/22C10 is a MAP1B-like protein required for dendritic and axonal development. *Neuron* **26**, 357-370.
- Inbal, A., Levanon, D. and Salzberg, A. (2003). Multiple roles for *u-turn/ventral veinless* in the development of *Drosophila* PNS. *Development* **130**, 2467-2478.
- Knoll, B. and Drescher, U. (2002). Ephrin-As as receptors in topographic projections. *Trends Neurosci.* **25**, 145-149.
- Kolodziej, P. A., Timpe, L. C., Mitchell, K. J., Fried, S. R., Goodman, C. S., Jan, L. Y. and Jan, Y. N. (1996). *frazzled* encodes a *Drosophila* member of the DCC immunoglobulin subfamily and is required for CNS and motor axon guidance. *Cell* **87**, 197-204.
- Kraut, R. and Zinn, K. (2004). Roundabout 2 regulates migration of sensory neurons by signaling in *trans*. *Curr. Biol.* **14**, 1319-1329.
- Kruger, R. P., Aurandt, J. and Guan, K. L. (2005). Semaphorins command cells to move. *Nat. Rev. Mol. Cell Biol.* **6**, 789-800.
- Kühnlein, R. P. and Schuh, R. (1996). Dual function of the region-specific homeotic gene *spalt* during *Drosophila* tracheal system development. *Development* **122**, 2215-2223.
- Merritt, D. J. and Whittington, P. M. (1995). Central projections of sensory neurons in the *Drosophila* embryo correlate with sensory modality, soma position, and proneural gene function. *J. Neurosci.* **15**, 1755-1767.
- Mitchell, K. J., Doyle, J. L., Serafini, T., Kennedy, T. E., Tessier-Lavigne, M., Goodman, C. S. and Dickson, B. J. (1996). Genetic analysis of *netrin* genes in *Drosophila*: Netrins guide CNS commissural axons and peripheral motor axons. *Neuron* **17**, 203-215.
- Patel, N. H. (1994). Imaging neuronal subsets and other cell types in whole-mount *Drosophila* embryos and larvae using antibody probes. *Methods Cell Biol.* **44**, 445-487.
- Patel, N. H. (1996). *In situ* hybridization to whole-mount *Drosophila* embryos. In *A Laboratory Guide to RNA: Isolation, Analysis and Synthesis*, (ed. P. Krieg), pp. 357-370. New York: Wiley-Liss.
- Patel, N. H., Hayward, D. C., Lall, S., Pirkel, N. R., DiPietro, D. and Ball, E. E. (2001). Grasshopper *hunchback* expression reveals conserved and novel aspects of axis formation and segmentation. *Development* **128**, 3459-3472.
- Rusten, T. E., Cantera, R., Urban, J., Technau, G., Kafatos, F. C. and Barrio, R. (2001). Spalt modifies EGFR-mediated induction of chordotonal precursors in the embryonic PNS of *Drosophila* promoting the development of oenocytes. *Development* **128**, 711-722.
- Steigemann, P., Molitor, A., Fellert, S., Jackle, H. and Vorbruggen, G. (2004). Heparan sulfate proteoglycan syndecan promotes axonal and myotube guidance by slit/robo signaling. *Curr. Biol.* **14**, 225-230.
- Vaessin, H., Grell, E., Wolff, E., Bier, E., Jan, L. Y. and Jan, Y. N. (1991). *Prospero* is expressed in neuronal precursors and encodes a nuclear protein that is involved in the control of axonal outgrowth in *Drosophila*. *Cell* **67**, 941-953.
- VanZomeran-Dohm, A., Flannery, E. and Duman-Scheel, M. (2008). Whole-mount in situ hybridization detection of mRNA in GFP-marked *Drosophila* imaginal disc mosaic clones. *Fly (Austin)* **2**, 323-325.
- von Hilchen, C. M., Beckervordersandforth, R. M., Rickert, C., Technau, G. M. and Altenhein, B. (2008). Identity, origin, and migration of peripheral glial cells in the *Drosophila* embryo. *Mech. Dev.* **125**, 337-352.
- Wang, B., Xiao, Y., Ding, B. B., Zhang, N., Yuan, X., Gui, L., Qian, K. X., Duan, S., Chen, Z., Rao, Y. et al. (2003). Induction of tumor angiogenesis by Slit-Robo signaling and inhibition of cancer growth by blocking Robo activity. *Cancer Cell* **4**, 19-29.